

## Theory of structural trends within the sp bonded elements

This article has been downloaded from IOPscience. Please scroll down to see the full text article.

1991 J. Phys.: Condens. Matter 3 495

(<http://iopscience.iop.org/0953-8984/3/5/001>)

View [the table of contents for this issue](#), or go to the [journal homepage](#) for more

Download details:

IP Address: 171.66.16.151

The article was downloaded on 11/05/2010 at 07:04

Please note that [terms and conditions apply](#).

## Theory of structural trends within the sp bonded elements

J C Cressoni† and D G Pettifor

Department of Mathematics, Imperial College of Science, Technology and Medicine,  
London SW7 2BZ, UK

Received 21 August 1990

**Abstract.** A simple nearest neighbour orthogonal tight binding model is shown to explain qualitatively the observed trends in structural stability within the sp bonded elements. The relative stabilities were predicted by comparing the band energies directly, using the structural energy difference theorem to prepare the bond lengths of the different structure types appropriately. This allows the structural trends to be interpreted in terms of the topology of the local atomic environment through the behaviour of the first few moments of the densities of states.

### 1. Introduction

The sp bonded elements show a broad range of crystal structure (see, for example, Donohue 1974). The first three groups (I, II and III) usually take the close-packed metallic structure types: face centred cubic (FCC), hexagonal close packed (HCP), or body centred cubic (BCC). The elements of group IV show the trend from three-fold co-ordinated graphite through four-fold co-ordinated diamond to twelve-fold co-ordinated FCC on moving down the column from carbon through silicon, germanium and tin to lead. Apart from the dimeric form of nitrogen, the group V pnictides take structures based on the stacking of three-fold co-ordinated buckled layers of atoms, whereas the group VI chalcogenides take structures based on two-fold co-ordinated helical chains. The group VII halogens crystallize as dimers which are held together on the lattice by very weak van der Waals interactions.

Allan and Lannoo (1983) have shown that the nearest neighbour (NN) orthogonal tight binding (TB) approximation can predict the general structural features which are observed across the periodic table. Their predictions were made by computing the total binding energy curves for a given sp bonded element with respect to the different lattices, and then comparing the resultant binding energies at the theoretical equilibrium separations. Their figure 7 shows the correct trend as a function of group number from close-packed metallic structures, through the four-fold co-ordinated diamond, the three-fold co-ordinated buckled layer and the two-fold co-ordinated helical chain to the singly co-ordinated dimer. In this paper we focus *directly* on the very small differences in

† Present address: Departamento de Física, Universidade Federal de Alagoas, Cidade Universitária, CEP 57061 Maceió (AL), Brazil.

energy between the different structure types by using the structural energy difference theorem (Pettifor 1986). This gives the difference in energy between two structures as the difference in their *attractive* band energies once the bond lengths have been adjusted to show the same *repulsive* energy. This allows the structural trends to be interpreted in terms of the topology of the local atomic environment through the behaviour of the first few moments of the densities of states.

The plan of this paper is as follows. In section 2 we outline the TB model and show how the hopping or bond integrals are fixed by the structural energy difference theorem. In section 3 we examine the relative stabilities of structures with NN co-ordinations ranging from  $z = 1$  (dimer),  $z = 2$  (zig-zag chain),  $z = 3$  (single graphitic layer or honeycomb lattice),  $z = 4$  (both diamond cubic and diamond hexagonal), through to  $z = 12$  (both close packed cubic and hexagonal). In addition we will consider the BCC lattice with  $z = 14$  corresponding to eight first- and six second-NNS. In section 4 we interpret the broad structural trends in terms of the behaviour of the third and fourth moments of the densities of states. In section 5 we conclude.

## 2. The tight binding model

The total binding energy per atom of an elemental sp-bonded system may be written within the TB approximation as the sum of three terms, namely

$$U = U_{\text{rep}} + U_{\text{bond}} + U_{\text{prom}} \quad (1)$$

The repulsive energy  $U_{\text{rep}}$  is assumed to be pairwise in character (Ducastelle 1970), so that

$$U_{\text{rep}} = \frac{1}{2N} \sum_{i,j}' \varphi(R_{ij}) \quad (2)$$

where  $N$  is the number of atoms in the system. The attractive covalent bond energy  $U_{\text{bond}}$  is usually evaluated within the two-centre orthogonal TB approximation (Slater and Koster 1954). For the case in which all sites are equivalent and the crystal field shifts are orbital-independent

$$U_{\text{bond}} = \sum_{\alpha=s,p} \int^{\epsilon_F} (\epsilon - \epsilon_{\alpha}) n_{\alpha}(\epsilon) d\epsilon \quad (3)$$

where  $n_{s,p}(\epsilon)$  are the local s, p electronic density of states,  $\epsilon_{s,p}$  are the effective s, p atomic energy levels, and  $\epsilon_F$  is the Fermi energy. The promotion energy  $U_{\text{prom}}$  is driven by the change in relative s : p occupancy and is given by

$$U_{\text{prom}} = (\epsilon_p - \epsilon_s) \Delta N_p \quad (4)$$

where  $\Delta N_p$  is the change in the number of p electrons on bringing the reference atoms together to form the bond. We should note that in practice equation (1) gives the binding energy with respect to some *reference* free atom state which usually differs from the *true* atomic ground state due to, for example, the neglect of spin-polarization or the shift in atomic energy levels arising from the renormalization of the wavefunctions in the bonding situation (see, for example, Sankey and Niklewski 1989).

The form of equation (1) may be justified from first principles by working within the Harris-Foulkes approximation (Harris 1985, Foulkes and Haydock 1989) to density

functional theory (see, for example, Sutton *et al* 1988 and references therein). It is important to realize that the usual crystal field shifts in the atomic energy levels have been removed from the *band* energy

$$U_{\text{band}} = \sum_{\alpha=s,p} \int^{\varepsilon_F} \varepsilon n_{\alpha}(\varepsilon) d\varepsilon \quad (5)$$

and grouped together with the first term  $U_{\text{rep}}$  (Allan and Lannoo 1983, Pettifor 1990). The remaining bond and promotion energies depend only on the electronic energies relative to  $\varepsilon_s$  and  $\varepsilon_p$ . The energy difference  $\varepsilon_{sp} = \varepsilon_s - \varepsilon_p$  is itself assumed to be environment independent, the crystal field effects giving a uniform shift in the on-site energy levels. It then follows from equations (3)–(5) that the *change* in the bond and promotion energies on going from one structure type to another is simply equivalent to the change in the band energy under the constraint that the atomic energy levels  $\varepsilon_s$  and  $\varepsilon_p$  are not renormalized but are kept frozen, i.e.

$$\Delta U_{\text{bond}} + \Delta U_{\text{prom}} = (\Delta U_{\text{band}})_{\Delta\varepsilon_{s,p}=0}. \quad (6)$$

This is consistent with the force theorem of Pettifor (1976, 1978) and Andersen (1980) and the frozen potential theorem of Pettifor and Varma (1979).

The two-centre TB hopping integrals have been assumed to take the following simple form

$$\left. \begin{array}{l} s\sigma(R) \\ p\sigma(R) \\ p\pi(R) \\ s\sigma(R) \end{array} \right\} = \left. \begin{array}{l} -1.00 \\ 2.31 \\ -0.76 \\ 1.31 \end{array} \right\} h(R) \quad (7)$$

so that they display the same functional dependence on interatomic distance, namely  $h(R)$ . This is, of course, only a first approximation, as the angular character of the orbitals can lead to quite different distance dependences for the  $\sigma$  and  $\pi$  bonds (see, for example, figure 4 of Allen *et al* 1986). The ratio  $s\sigma:p\sigma:p\pi:s\sigma$  implicit in equation (7) has been chosen equal to Harrison's (1980) solid-state table values except for  $p\pi$  which has been increased by 30%. This increase in  $p\pi$  was found necessary in order to stabilize the close-packed structures with respect to the dimer for the case of the alkali metals with  $N = 1$  (Cressoni 1989).

The *explicit* form of the distance dependence  $h(R)$  is not required within the present NN model since we are using the structural energy difference theorem (Pettifor 1986, section 7 Pettifor 1987) to predict the relative stability of the different structure types. This theorem states that the total energy difference  $\Delta U$  between two systems in equilibrium under a binding-energy law of the type given in equation (1) is, to first order in  $\Delta U/U$ ,

$$\Delta U = (\Delta U_{\text{bond}} + \Delta U_{\text{prom}})_{\Delta U_{\text{rep}}=0}. \quad (8)$$

That is, the total energy difference is the difference in the bond plus promotion energies provided the bond lengths have been adjusted so that the two lattices have identical repulsive energies. It follows from equations (6) and (8) that

$$\Delta U = (\Delta U_{\text{band}}(\varepsilon_s, \varepsilon_p))_{\Delta U_{\text{rep}}=0} \quad (9)$$

where the band energy is evaluated for the two lattices with the same values of the atomic

energy levels  $\varepsilon_s$  and  $\varepsilon_p$ . Thus, equation (9) generalizes the frozen potential theorem (Pettifor and Varma 1979) to the case in which the lattices have different local co-ordination and hence different NN bond lengths.

The pairwise repulsive potential  $\varphi(R)$  has been taken to vary as the square of the hopping integrals (Pettifor and Podlucky 1986), i.e.

$$\varphi(R) = Ah^2(R) \quad (10)$$

where  $A$  is a constant. This approximation appears to be a reasonable assumption for sp-bonded systems. For example, Goodwin *et al* (1989) have recently fitted the local density functional binding energy curves of diamond,  $\beta$ -Sn, sc and FCC silicon (Yin and Cohen 1982) with a short-ranged two-centre orthogonal TB model in which  $\varphi(R) \propto [h(R)]^{2.27}$ .

The assumption of equation (10) allows us to write the total energy difference in the form

$$\Delta U = (\Delta U_{\text{band}}(\varepsilon_s, \varepsilon_p))_{\Delta\mu_2=0} \quad (11)$$

where  $\mu_2$  is the second-moment of the local density of states, namely

$$\mu_2 = \int_{-\infty}^{\infty} \varepsilon^2(n_s(\varepsilon) + n_p(\varepsilon)) d\varepsilon. \quad (12)$$

This follows since the second moment may be expressed in terms of all paths of length two which start from and end on a given atom (Cyrot-Lackmann 1968), so that

$$\Delta\mu_2 \propto \Delta \left( \sum_{R \neq 0} h^2(R) \right) \propto \Delta U_{\text{rep}}. \quad (13)$$

The constraint  $\Delta\mu_2 = 0$  fixes the relative values of the hopping integrals between the different structure-types. Taking the simple cubic lattice with  $\bar{z} = 6$  as reference with an equilibrium NN integral  $h_{11}$ , we have from equation (13) that the appropriate hopping integral for any other lattice with co-ordination  $\bar{z}$  is given by

$$h_{\bar{z}} = (6/\bar{z})^{1/2} h_{11}. \quad (14)$$

Thus, we now have the necessary hopping integrals to predict the relative stabilities of different NN structure-types directly from equation (11) for any given choice of  $\varepsilon_{sp} = \varepsilon_s - \varepsilon_p$ . For the BCC lattice with eight first- and six second-NNS we have chosen  $h(R_2)/h(R_1) = 0.33$  as found by the localized TB scheme of Andersen and Jepsen (1984).

### 3. Crystal structure trends

The ground-state structures of the sp-bonded elements are shown in table 1. The alkaline earths Ca, Sr, Ba and Ra have been excluded as their structural stability is strongly influenced by the proximity of the transition metal d band (Skriver 1982). The grouping of Be and Mg with Zn, Cd and Hg is suggested by the phenomenological structure maps for binary compounds (Pettifor 1988). We see the well known trend from close-packed metallic co-ordination for  $N = 1, 2$ , and 3 (excluding hydrogen) to the open non-metallic structures for  $N = 5, 6$  and 7. In this paper we will examine the relative stabilities of structures with NN co-ordinations ranging from  $\bar{z} = 1$  (dimer),  $\bar{z} = 2$  (zig-zag chain with

**Table 1.** The ground-state structures of the sp bonded elements (Donohue 1974, Hafner 1989). (dimer), (octomer), (chain) or (layer) indicates that the structure comprises dimers, octomers, helical chains or buckled layers weakly bound together in the solid.

1	2	3	4	5	6	7
H (dimer)						
Li HCP	Be HCP	B complex	C graphite	N (dimer)	O (dimer)	F (dimer)
Na HCP	Mg HCP	Al FCC	Si DIA	P (layer)	S (octomer)	Cl (dimer)
K BCC	Zn HCP	Ga complex	Ge DIA	As (layer)	Se (chain)	Br (dimer)
Rb BCC	Cd HCP	In FCT	Sn DIA	Sb (layer)	Te (chain)	I (dimer)
Cs BCC	Hg BCT	Tl HCP	Pb FCC	Bi (layer)	Po sc	At (dimer)

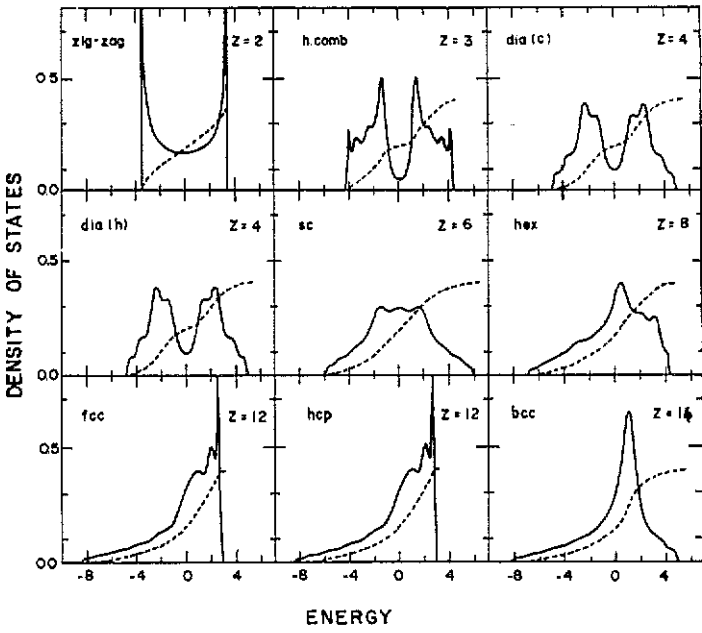
90° bond angles),  $z = 3$  (single graphitic layer or honeycomb lattice),  $z = 4$  (both diamond-cubic and diamond-hexagonal lattices),  $z = 6$  (simple cubic),  $z = 8$  (simple hexagonal), through to  $z = 12$  (both CCP and ideal HCP lattices). In addition we will consider the BCC lattice with  $z = 14$  corresponding to eight first- and six second-nns.

Figures 1–3 show the pure s, pure p and hybridized sp (with  $\epsilon_s = \epsilon_p = 0$ ) densities of states for these different co-ordinations using the TB hopping integrals defined by equations (7) and (14). The energy is in units of  $h_0$  throughout so that the SC s-band in figure 1, for example, runs from  $-6$  to  $+6$ . The density of states was calculated using the recursion method of Haydock *et al* (1972, 1975) to nine exact levels. The continued fraction was terminated with the square-root terminator for the case of a continuous spectrum or the Turchi *et al* (1982) terminator for the case of a single band gap. The band edges were chosen using the optimized prescription of Beer and Pettifor (1984) which may be generalized to the case of a single band gap (Beer 1985, Cressoni 1989). The densities of states for the zig-zag chain in figures 2 and 3 were evaluated using the Turchi *et al* (1982) terminator for a double band gap, and display distinct bonding, non-bonding and anti-bonding bands. It is interesting to note that the pure s bands for the cubic and hexagonal diamond or close-packed lattices are identical as they have identical moments, which has been proved by Burdett and Lee (1985). It is the angular character of the valence orbitals which distinguishes between cubic and hexagonal systems within a NN TB model.

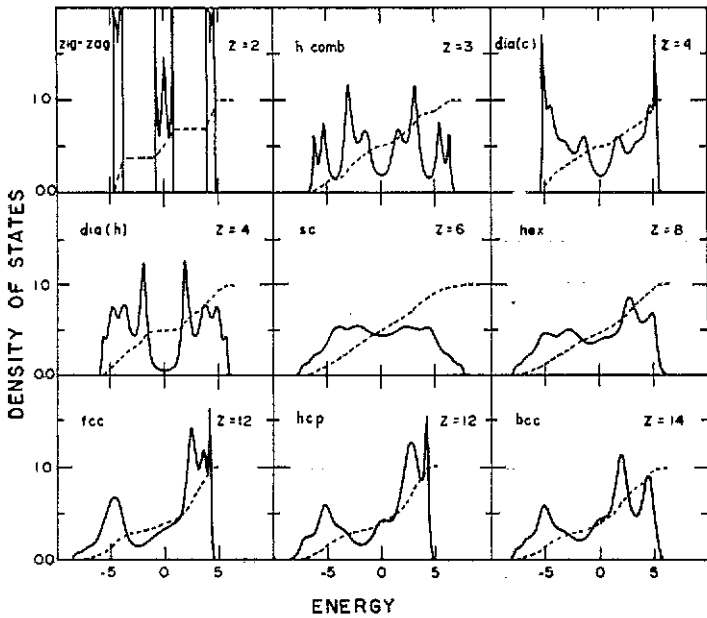
In order to study the influence of the atomic energy level separation  $\epsilon_{sp}$  on the relative structural stability, we have calculated the densities of states for values of

$$\hat{\epsilon}_{sp} = \epsilon_{sp}/W_0 = -\tan(m\pi/2) \quad (15)$$

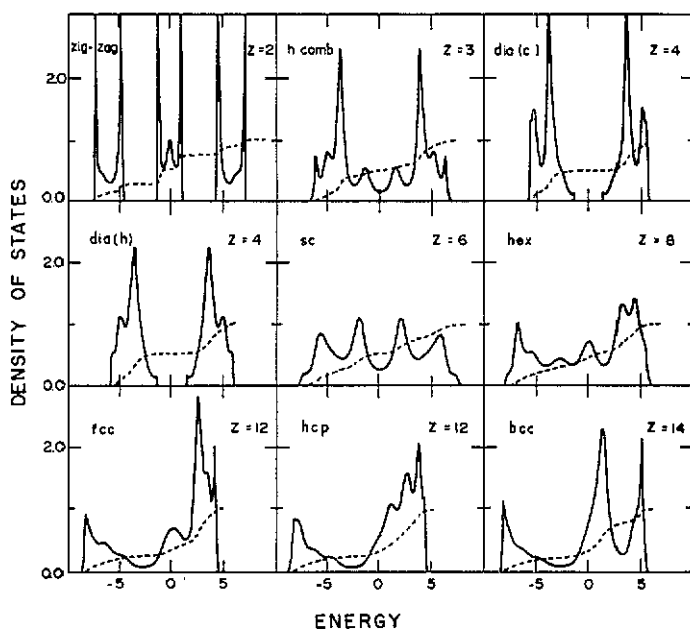
with  $m = 0.2, 0.4, 0.6, 0.8$  and  $1.0$ , where  $W_0$  is the simple cubic s bandwidth, namely  $W_0 = 12h_0$ . Figure 4 shows the resultant densities of states for  $m = 0.2, 0.4$  and  $0.6$  corresponding to  $\hat{\epsilon}_{sp} = -0.32, -0.73$  and  $-1.38$  respectively. We see that for the largest atomic energy level separation a gap has opened up between the s and p bands in all



**Figure 1.** The *s* density of states for the different lattices in energy units of  $\hbar\omega_0$ . The broken curves give the integrated density of states provided the numbers on the vertical scale are multiplied by five.



**Figure 2.** The *p* density of states for the different lattices in energy units of  $\hbar\omega_0$ . The broken curves give the integrated density of states provided the numbers on the vertical scale are multiplied by six.



**Figure 3.** The *sp* density of states for the different lattices in energy units of  $h_0$  with  $\epsilon_{sp} = 0$ . The broken curves give the integrated density of states provided the numbers on the vertical scale are multiplied by eight.

structures. Interestingly the *sp* hybridization gap in the diamond lattice, which is seen in the upper panel of figure 4, is destroyed by the increased *sp* energy level separation in the middle panel, before a gap reappears between the *s* and *p* band in the lower panel. The densities of states for  $m = 1.0$ , corresponding to infinite *sp* energy level separation, are given by the pure *s* and pure *p* bands in figures 1 and 2 respectively.

Figures 5 and 6 show the structural energy as a function of band filling for the different structure types. We have defined the structural energy as the difference between the band energy for a given structure and that corresponding to a *reference* skew-rectangular density of states, whose first three moments  $\mu_0$ ,  $\mu_1$  and  $\mu_2$  are fixed by the structural energy difference theorem through equations (11)–(14) and  $\mu_3$  is chosen equal to that for the *sc* lattice. Comparing the band energies with the skew-rectangular reference allows the very small energy differences between the different structure types to be displayed more clearly. We should, however, note that for the case  $\hat{\epsilon}_{sp} = -1.38$ , where the *s* and *p* bands have split apart, a *single* skew-rectangular band with the appropriate  $\mu_3/\mu_2^{3/2}$  is not possible and we have therefore taken the average band energy of all the different structures as reference. The *BCC* structural energy curves, corresponding to  $h(R_2)/h(R_1) = 0.33$ , follow the curves for the close-packed structures. However, since they nowhere have the lowest energy, we have omitted them from figures 5 and 6 for clarity.

The lower panel of figure 7 shows the *predicted* domains of structural stability within an  $(\hat{\epsilon}_{sp}, N)$  structure map. For  $\hat{\epsilon}_{sp} = 0$  we see the structure trends from *FCC*  $\rightarrow$  *HCP*  $\rightarrow$  *FCC*  $\rightarrow$  *HEX*  $\rightarrow$  honeycomb  $\rightarrow$  diamond cubic  $\rightarrow$  honeycomb  $\rightarrow$  simple cubic  $\rightarrow$  zig-zag  $\rightarrow$  dimer which correlates with the structural energy curves of



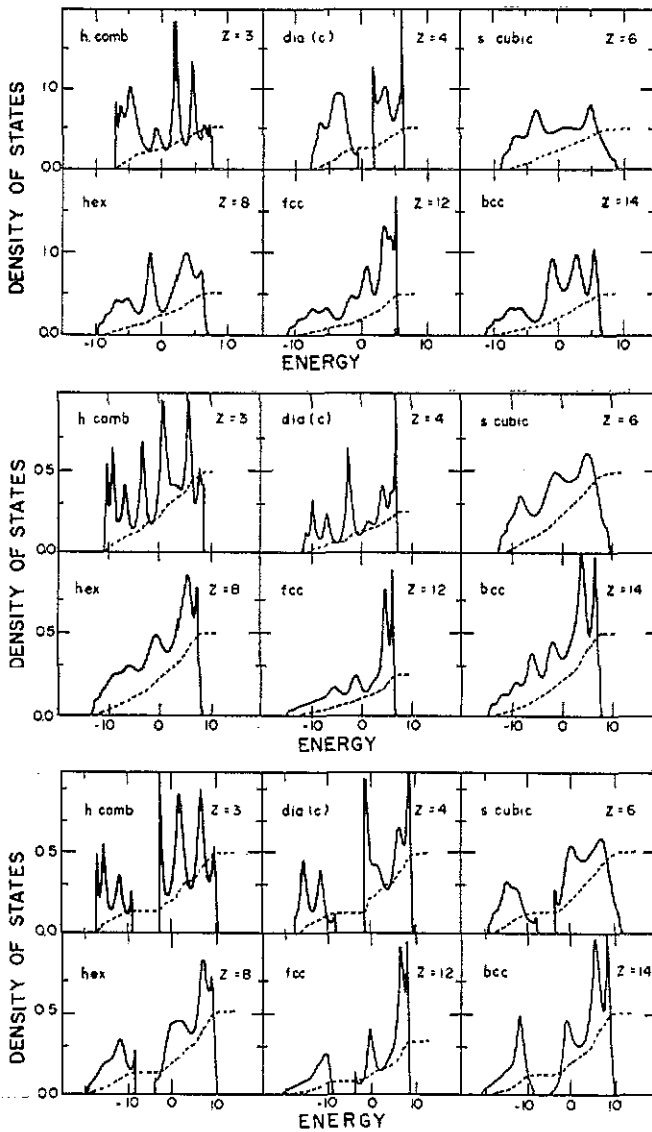


Figure 4. The  $sp$  density of states for the different lattices in energy units of  $h_0$  for  $\epsilon_{sp} = -0.32$  (upper panel),  $-0.73$  (middle panel) and  $-1.38$  (lower panel) respectively. The diamond cubic and FCC densities of states for  $\epsilon_{sp} = -0.73$  have been reduced by a factor of two and the FCC density of states for  $\epsilon_{sp} = -1.38$  by a factor of 1.5 in order to fit them within the appropriate boxes. The broken curves give the integrated density of states provided the numbers on the vertical scale are multiplied by sixteen.

figure 5. For  $\hat{\epsilon}_{sp} = -\infty$  we see the trend from close-packed  $\rightarrow$  zig-zag  $\rightarrow$  dimer  $\rightarrow$  zig-zag  $\rightarrow$  SC  $\rightarrow$  FCC  $\rightarrow$  HCP  $\rightarrow$  FCC  $\rightarrow$  diamond hexagonal  $\rightarrow$  diamond cubic  $\rightarrow$  zig-zag  $\rightarrow$  simple cubic  $\rightarrow$  dimer  $\rightarrow$  SC. This correlates with the predictions of figure 5 for the pure  $s$  band from  $N$  equals 0  $\rightarrow$  2 and for the pure  $p$  band from  $N$  equals 2  $\rightarrow$  8.

The upper panel of figure 7 shows the *experimental* ground state structures of the  $sp$ -bonded elements within a  $(\hat{\epsilon}_{sp}, N)$  structure map. The values of the atomic energy level

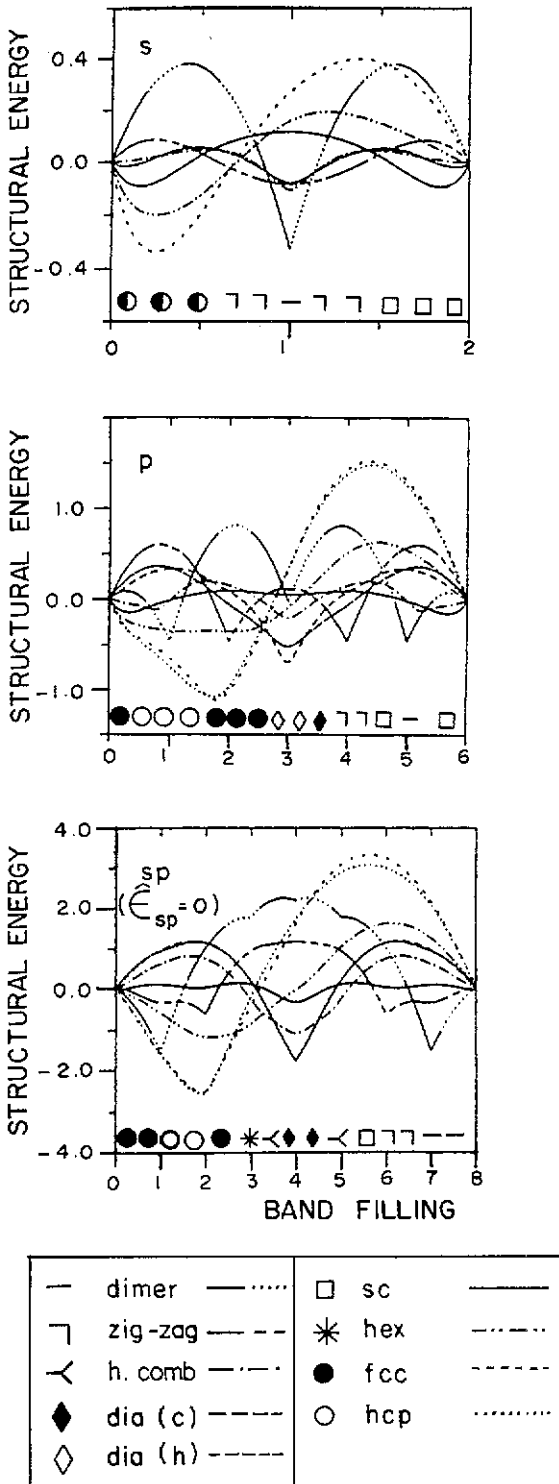
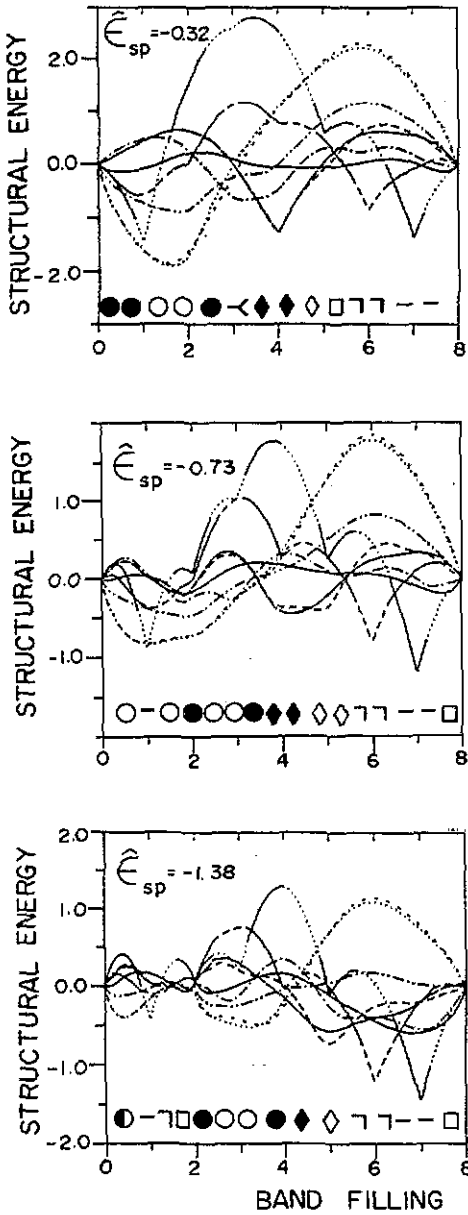
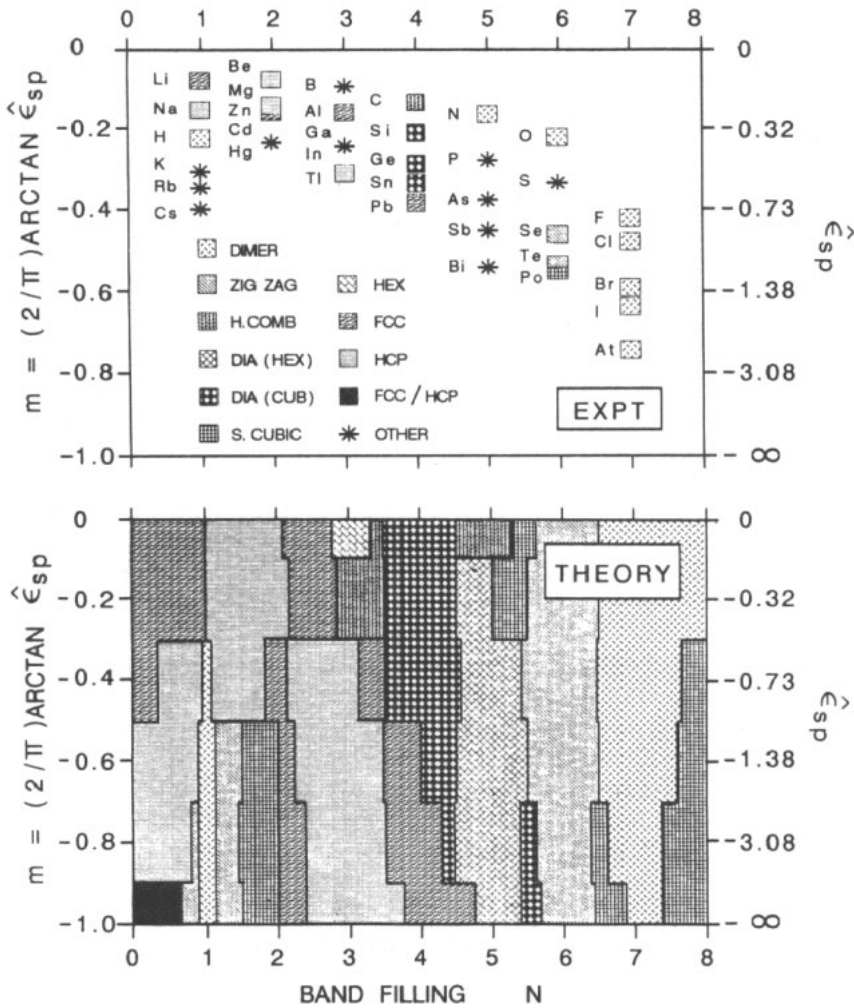


Figure 5. The structural energy in units of  $h_0$  as a function of band filling for the pure s, pure p, and sp ( $\epsilon_{sp} = 0$ ) cases.



—	dimer	— · · · · ·	□	sc	—
└┘	zig-zag	— — — — —	*	hex	— · · · · ·
└┘	h. comb	— · · · · ·	●	fcc	— — — — —
◆	dia (c)	— — — — —	○	hcp	· · · · ·
◇	dia (h)	— — — — —			

**Figure 6.** The structural energy in units of  $h_0$  as a function of band filling for  $\epsilon_{sp} = -0.32$  (upper panel),  $-0.73$  (middle panel) and  $-1.38$  (lower panel) respectively.



**Figure 7.** A comparison of theoretical (lower panel) and experimental (upper panel) structure maps of the *sp* bonded elements.

difference  $\epsilon_{sp}$  were taken from Herman and Skillman (1963) with relativistic corrections included. The values of  $W_0$ , the pure *s* band width with respect to the SC lattice, were estimated using Harrison's (1980) universal form for the *ss* $\sigma$  hopping integral, namely

$$ss\sigma = -h(R) = -2.80/R^2 \text{ Ryd.} \quad (16)$$

It then follows from equation (14) that

$$W_0 = 12h_0 = 12(\zeta/6)^{1/2}h(R_\zeta) = 13.7\zeta^{1/2}/R_\zeta^2 \text{ Ryd} \quad (17)$$

where  $R_\zeta$  is the observed NN distance for a given element with local co-ordination  $\zeta$ . This simple expression gives a qualitative estimate of the *s* band width of all the *sp*-bonded elements except hydrogen. In the latter case we have taken  $W_0$  equal to the

2.5 Ryd which was evaluated recently by Skinner and Pettifor (1990) for hydrogen with respect to the sc lattice.

Figure 7 shows that the theory predicts some of the broad features displayed by the experimental structure map. In particular, beginning on the right hand side of the figure where the assumptions of the TB model are most appropriate, we see that the theory correctly predicts that the most stable structures of the halogens are built from dimers, whereas those of the chalcogens are based on zig-zag linear chains (see, for example, figure 3.12 of Harrison 1980). The exceptions are oxygen with its dimeric behaviour and polonium with its sc structure (sulphur exhibits structures based on helical chains at high temperatures). Nevertheless, we see that both dimeric and sc domains adjoin the theoretical zig-zag domain centred on  $N = 6$ . Relaxation of the simplifying constraint that the repulsive pair potential varies as the square of the hopping integrals (see equation (10)) would change the theoretical predictions, a softer repulsive term favouring lower co-ordinations, a harder repulsive term favouring higher co-ordinations (Abell 1985).

The theoretical predictions for the pnictides with  $N = 5$  are very poor, although the curves do predict the *three*-fold co-ordinated honeycomb (or graphite) lattice for small values of  $\hat{\epsilon}_{sp}$ . In retrospect a *buckled* three-fold co-ordinated layer should have been used for comparison rather than the *planar* honeycomb lattice (see, for example, figure 8 of Allan and Lannoo 1983). The dimeric form of nitrogen, like oxygen, is probably related to the relative steepness of the repulsive interaction to that of the hopping integrals.

The group IVB elements are predicted to change from the open *four*-fold co-ordinated diamond cubic structure to the close-packed *twelve*-fold co-ordinated FCC structure as  $\hat{\epsilon}_{sp}$  becomes increasingly negative. This is consistent with the observation that silicon, germanium and tin are diamond cubic whereas lead is FCC. The latter has a larger negative value of  $\epsilon_{sp}$  due to a 3 eV relativistic contribution (Herman and Skillman 1963) which weakens the strength of the  $sp^3$  hybrids due to a sizeable positive promotion energy (see equation (4)). Again the 2p element is exceptional, carbon taking the graphite structure. Nevertheless, theoretically there are three-fold co-ordinated honeycomb domains neighbouring the large diamond cubic domain centred on  $N = 4$ .

Even though the  $sp$ -bonded metals with  $N = 1, 2$  and 3 are not expected to be described accurately by a NN orthogonal TB model, we see that the simple theory predicts correctly the occurrence of close-packed structures in this region. Moreover, the trend from HCP to FCC as  $N$  increases across a period from the alkali metals and the trend from FCC to HCP as  $\hat{\epsilon}_{sp}$  becomes more negative down group IIIB is well reproduced. Note, however, that the alkali metals potassium, rubidium and caesium are BCC, not HCP, a fact which has been related to the presence of the d-band just above the Fermi energy (Skriver 1982). For large negative values of  $\hat{\epsilon}_{sp}$  we expect the dimer to be most stable for  $N = 1$  as the  $s$  bonding dominates, in agreement with the upper panel of figure 5. However, looking at figure 7, the dimeric form of hydrogen is probably also related to a softer repulsive core than that assumed by  $\varphi(R) \propto [h(R)]^2$  in the present theory (Abell 1985).

#### 4. Interpretation in terms of moments

The broad behaviour of the theoretical structural energy curves in figures 5 and 6 can be understood in terms of the moments of the local density of states (see, for example, Cyrot-Lackmann 1968, Ducastelle and Cyrot-Lackmann 1971, Turchi and Ducastelle

1985, Burdett and Lee 1985 and Ducastelle 1990 and references therein). As is well known, the  $n$ th moment  $\mu_n$  of the density of states associated with a given atom can be related directly to the sum of all paths of length  $n$  which start from and end on that atom.

This is a very powerful result. For example, it immediately implies that all lattices which contain only even-membered rings will have all their odd moments vanishing so that the resultant densities of states must be symmetric (assuming no on-site hopping contributions which is true for  $\varepsilon_s = 0$ ,  $\varepsilon_p = 0$  or  $\varepsilon_{sp} = 0$ ). This explains the symmetric behaviour of the densities of states in figures 1, 2 and 3 for the zig-zag, honeycomb, diamond and sc lattices which contain only even-membered rings. We see, on the other hand, that the hexagonal, FCC, HCP and BCC lattices have densities of states skewed to lower energies due to the presence of the odd three-membered rings and non-vanishing third moments  $\mu_3$ . This accounts for the asymmetric behaviour of the close-packed and hexagonal structural energy curves in figure 5. Thus, we have the important result that the CP structures are more stable than the more open structures for less than half-full bands due to the presence of three-membered rings which are absent in the latter structure types.

The relative stability of different structure types with even-membered rings can sometimes be inferred by looking at the relative strengths of their normalized fourth moments  $\hat{\mu}_4 = \mu_4/\mu_2^2$ . In table 2 we show the different types of paths which contribute to the fourth moment of the different lattices including the 2D square lattice for later comparison with the three-dimensional diamond lattice. We can write the fourth moment with respect to a given site as

$$\mu_4 = \sum_i n_i \mu_{4,i} \quad (18)$$

where  $i$  runs over all the different types of four-path contributions about that site, and  $n_i$  and  $\mu_{4,i}$  give the number of such contributions and the corresponding fourth moment respectively. For example, on the three-fold co-ordinated honeycomb lattice there are two types of contribution, the one ( $i = 1$ ) corresponding to four hops back and forth between neighbouring pairs, the other ( $i = 2$ ) corresponding to four hops between three atomic neighbours. It is easy to see that the former enters three times so that  $n_1 = 3$ , whereas the latter enters twelve times so that  $n_2 = 12$ , as given in table 2.

For the case of *angularly independent* s orbitals all types of paths have the same weight  $ss\sigma^4$  so that from equation (18)

$$\hat{\mu}_4^s = \left( \sum_i n_i \omega_i \right) / \bar{\omega}^2 \quad (19)$$

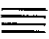
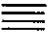

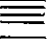
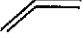
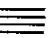


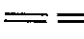


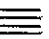
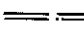


where the normalized weight of each path is unity and is thus independent of distance or structure type. Summing the non-ring paths we have

$$\hat{\mu}_4^s = (2 - 1/\bar{\omega}) + \hat{\mu}_{4,\text{ring}}^s \quad (20)$$

where the second term on the right hand side represents the ring contributions to the normalized fourth moment. In figure 8 we plot  $\hat{\mu}_4$  versus  $\bar{\omega}$  for the different lattices. We see that for the s orbital case  $(2 - 1/\bar{\omega})$  is the sole contribution for the dimer, zig-zag, honeycomb and diamond lattices, the large deviation from the dotted curve for the square, sc, hexagonal and CP structures being due to the presence of four-membered ring terms (see table 2).

For the case of *angularly dependent* p orbitals the weight  $\mu_{4,i}$  is a function not only of the hopping integrals but also of the type of path  $i$ . If  $\theta_i$  is the relevant bond angle in the

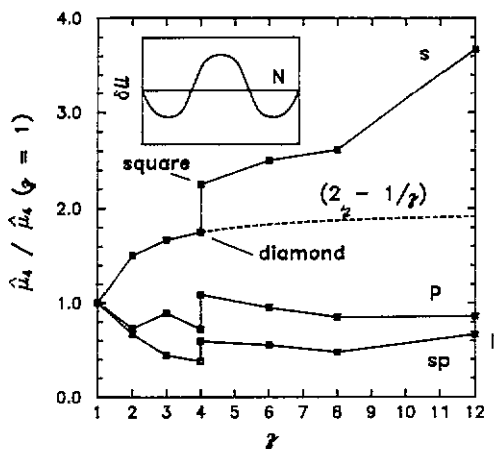
Table 2. Contributions to the normalized fourth moment  $\mu_4/\mu_4^2$  ( $\xi = 1$ ) where  $\mu_4 = \mu_4/\mu_2^2$  and  $\xi$  is the local co-ordination.  $n_i$  and  $w_i$ , which are defined after equations (18) and (22), give the number and normalized weight of the  $i$ th type of contribution to the fourth moment respectively. The numbers in brackets in the last three columns give the total s, p or sp normalized fourth moments for each structure type.

$\xi$	Type $i$	$n_i$	$w_i$			$n_i w_i / \xi^2$		
			s	p	sp	s	p	sp
1		1	1.000	1.000	1.000	1.000 (1.000)	1.000 (1.000)	1.000 (1.000)
2		2	1.000	1.000	1.000	0.500	0.500	0.500
		4	1.000	0.224	0.167	1.000 (1.500)	0.224 (0.724)	0.167 (0.667)
3		3	1.000	1.000	1.000	0.333	0.333	0.333
		12	1.000	0.418	0.079	1.333 (1.667)	0.557 (0.890)	0.105 (0.438)
4		4	1.000	1.000	1.000	0.250	0.250	0.250
		24	1.000	0.311	0.084	1.500 (1.750)	0.467 (0.717)	0.126 (0.376)
4		4	1.000	1.000	1.000	0.250	0.250	0.250
		8	1.000	1.000	0.211	0.500	0.500	0.106
		16	1.000	0.224	0.167	1.000	0.224	0.167
		8	1.000	0.224	0.134	0.500 (2.250)	0.112 (1.086)	0.067 (0.590)
6		6	1.000	1.000	1.000	0.167	0.167	0.167
		12	1.000	1.000	0.211	0.333	0.333	0.070
		48	1.000	0.224	0.167	1.333	0.299	0.223
		24	1.000	0.224	0.134	0.667 (2.500)	0.149 (0.948)	0.089 (0.549)

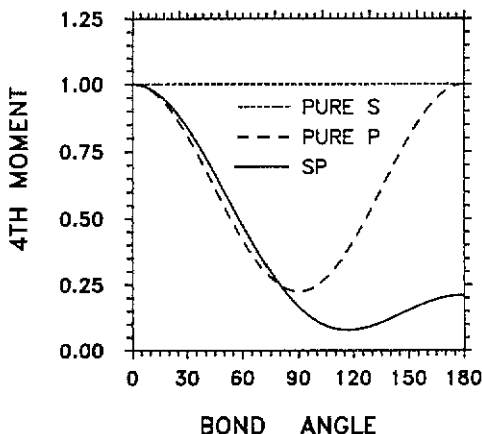
three atom contributions in table 2, then it follows from the angular dependence of the energy integrals in Slater and Koster (1954) that

$$\begin{aligned}
 \mu_{4,i} = & [ss\sigma^4 + sp\sigma^4 + pp\pi^4 + 2ss\sigma^2sp\sigma^2 + 2pp\pi^2(sp\sigma^2 + pp\sigma^2)] \\
 & + 2sp\sigma^2(ss\sigma^2 - 2ss\sigma pp\sigma + pp\sigma^2) \cos \theta_i \\
 & + [sp\sigma^4 + pp\sigma^4 + pp\pi^4 + 2sp\sigma^2pp\sigma^2 - 2pp\pi^2(sp\sigma^2 + pp\sigma^2)] \cos^2 \theta_i.
 \end{aligned}
 \tag{21}$$

Figure 9 shows the resultant angular dependence for the p and sp cases with  $\epsilon_{sp} = 0$ , which look very similar to the recent numerical results of Carlsson (1989) for the angular dependence of an effective three-body potential derived from p or  $sp^3$  hybrids. We see



**Figure 8.** The normalized fourth moment  $\hat{\mu}_4/\hat{\mu}_4$  ( $\zeta = 1$ ) versus the local co-ordination  $\zeta$  for the pure s, pure p, and sp ( $\epsilon_{sp} = 0$ ) cases. The dotted curve gives the s orbital result in the absence of ring terms. The inset shows the oscillatory behaviour of the energy difference between two structures with different fourth moments such that  $\delta\mu_4 > 0$ .



**Figure 9.** The angular dependence of the three-atom fourth moment contribution, equation (21), for the pure s, pure p, and sp ( $\epsilon_{sp} = 0$ ) cases.

that in the pure p case  $\mu_{4,i}$  has a minimum corresponding to  $90^\circ$ , whereas in the sp case the minimum is close to  $117^\circ$ . We will see that this is important for stabilizing the diamond structure with  $\theta = 109^\circ$  or the graphite structure with  $\theta = 120^\circ$  when the bands are half-full.

Finally, we can generalize expression (19) to the sp case by writing

$$\hat{\mu}_4/\hat{\mu}_4(\zeta = 1) = \left( \sum_i n_i \omega_i \right) / \zeta^2 \quad (22)$$

where  $\omega_i = \mu_{4,i}/\mu_{4,1}$ . It follows that the normalized weight  $\omega_i$  for the two atom contributions is unity, as shown in table 2. For the s case  $\hat{\mu}_4(\zeta = 1) = 1.0$  so that equations (19) and (22) are equivalent. Table 2 gives the corresponding normalized weights  $\omega_i$  for the different orbitals and types of path and their contributions to the sum in equation (22). Figure 8 shows that the angular dependence of the p orbitals severely decreases the value of  $\hat{\mu}_4/\hat{\mu}_4(\zeta = 1)$  compared with the s orbital case. In particular, we see that the four-fold co-ordinated diamond lattice has the lowest value of  $\hat{\mu}_4$  for both the p and sp cases, whereas the dimer had the lowest value for the pure s case.

The value of  $\mu_4$  reflects the shape of the density of states, in that a large value suggests a central peak or unimodal behaviour, whereas a small value suggests two well-separated peaks or bimodal behaviour (see, for example, figure 1 of Gaspard and Lambin 1985). This is illustrated by figure 1 for the s bands. As the local co-ordination  $\zeta$  increases,  $\mu_4$  increases rapidly and the densities of states clearly change from having a bimodal to a unimodal distribution. On the other hand, for the sp case as  $\zeta$  increases  $\mu_4$  decreases until a minimum is reached for the diamond lattice (see figure 8). We see in figure 3 that this corresponds to the opening up of a hybridization gap, thereby stabilizing the diamond lattice for a half-full band. Thus, if two lattices have different normalized fourth



moments, the lattice with the smaller moment will be the more stable for approximately half-full bands, whereas the lattice with the larger moment will be the more stable for nearly full or empty bands, as is illustrated schematically by the inset in figure 8.

The structural trends shown in figure 5 are *consistent* with the behaviour of the third and fourth moments. For less than half-full bands the CP structures are stabilized by the presence of three-membered rings. For more than half-full bands the trends from the dimer  $\rightarrow$  zig-zag chain  $\rightarrow$  SC for s orbitals, from diamond  $\rightarrow$  zig-zag chain  $\rightarrow$  SC  $\rightarrow$  dimer for p orbitals and from diamond  $\rightarrow$  honeycomb  $\rightarrow$  SC  $\rightarrow$  zig-zag for the sp orbitals are in the direction of increasing fourth moment. The higher moments are necessary, however, for predicting the precise shape of the curves in figure 5. In particular, the relative stability of the cubic versus hexagonal CP or diamond lattices requires a knowledge of  $\mu_5$  or  $\mu_6$  which can be seen from the fact that the cubic and hexagonal curves cross each other at least three or four times for the p and sp cases in figure 5 (Ducastelle and Cyrot-Lackmann 1971). Finally, the qualitative features of the theoretical structure map in figure 7 can be inferred by combining the predictions for  $\epsilon_{sp} = 0$  with those for the pure s and p bands corresponding to  $\epsilon_{sp} = -\infty$ .

## 5. Conclusions

A simple NN orthogonal TB model has provided a qualitative explanation of the observed trends in structural stability within the sp-bonded elements. The relative stabilities were predicted by comparing the band energies directly, once the bond lengths had been adjusted in accordance with the structural energy difference theorem. This allowed the structural trends to be interpreted in terms of the topology of the local atomic environment through the behaviour of the first few moments of the densities of states. In particular, the trend from CP to open structures across a period was seen to reflect the presence of the three-membered ring terms in the former structures and their absence in the latter. The normalized fourth moments were found to be very dependent on the angular character of the orbitals with important consequences for structural stability. For example, the dimer is the most stable structure for the half-full s orbital case, whereas the diamond lattice is the most stable structure for sp hybrids.

The simple model assumed that the repulsive pair potential varied with distance as the square of the hopping integrals. This constraint would have to be relaxed to account for the exceptions to the present theoretical predictions such as the occurrence of dimers for the 2p elements nitrogen and oxygen where softer repulsive cores are required. The model is currently being applied to d-bonded transition elements where a harder repulsive core is required in order to stabilize only CP structures across the entire series (Cressoni and Pettifor 1990).

## Acknowledgments

One of us (JCC) wishes to thank the Brazilian Agency Conselho Nacional de Desenvolvimento Científico e Tecnológico for financial support. It is a pleasure to thank Andrew Skinner and Roger Davies for helpful conversations.

## References

- Abell G C 1985 *Phys. Rev. B* **31** 6184
- Allan G and Lannoo M 1983 *J. Physique* **44** 1355
- Allen P B, Broughton J Q and McMahan A K 1986 *Phys. Rev. B* **34** 859
- Andersen O K 1980 *Electrons at the Fermi Surface* ed M Springford (Cambridge: Cambridge University Press) section 5.3
- Andersen O K and Jepsen O 1984 *Phys. Rev. Lett.* **53** 2571
- Beer N R 1985 *Ph.D. Thesis* University of London
- Beer N R and Pettifor D G 1984 *Electronic Structure of Complex Systems* ed P Phariseau and W Temmerman (New York: Plenum) p 769
- Burdett J K and Lee S 1985 *J. Am. Chem. Soc.* **107** 3063
- Carlsson A E 1989 *Atomistic Simulation of Materials: Beyond Pair Potentials* ed V Vitek and D J Srolovitz (New York: Plenum) p 103
- Cressoni J C 1989 *PhD Thesis* University of London
- Cressoni J C and Pettifor D G 1990 to be published
- Cyrot-Lackmann F 1968 *J. Phys. Chem. Solids* **29** 1235
- Donohue J 1974 *The Structure of the Elements* (New York: Wiley)
- Ducastelle F 1970 *J. Physique* **31** 1055
- 1991 *Order and Phase Stability in Alloys (Cohesion and Structure 3)* (Amsterdam: North-Holland)
- Ducastelle F and Cyrot-Lackmann F 1971 *J. Phys. Chem. Solid* **32** 285
- Foulkes W M C and Haydock R 1989 *Phys. Rev. B* **39** 12520
- Gasparid J P and Lambin P 1985 *The Recursion Method and Its Application (Solid State Sciences 58)* ed D G Pettifor and D L Weaire (Berlin: Springer) p 75
- Goodwin L, Skinner A J and Pettifor D G 1989 *Europhys. Lett.* **9** 701
- Hafner J 1989 *The Structures of Binary Compounds (Cohesion and Structure 2)* (Amsterdam: North-Holland) p 147
- Harris J 1985 *Phys. Rev. B* **31** 1770
- Harrison W A 1980 *Electronic Structure and the Properties of Solids* (San Francisco: Freeman)
- Haydock R, Heine V and Kelly M J 1972 *J. Phys. C: Solid State Phys.* **5** 2845
- 1975 *J. Phys. C: Solid State Phys.* **8** 2591
- Herman F and Skillman S 1963 *Atomic Structure Calculations* (New Jersey: Prentice Hall)
- Pettifor D G 1976 *Commun. Phys.* **1** 141
- 1978 *J. Chem. Phys.* **69** 2930
- 1986 *J. Phys. C: Solid State Phys.* **19** 285
- 1987 *Solid State Phys.* **40** 43
- 1988 *Mater. Sc. and Technol.* **4** 675
- 1990 *Many-Atom Interactions in Solids (Springer Proc. in Physics 48)* ed R M Nieminen, M J Puska and M Manninen (Berlin: Springer) p 64
- Pettifor D G and Podloucky R 1986 *J. Phys. C: Solid State Phys.* **19** 315
- Pettifor D G and Varma C M 1979 *J. Phys. C: Solid State Phys.* **12** L253
- Sankey O F and Niklewski D J 1989 *Phys. Rev. B* **40** 3979
- Skinner A J and Pettifor D G 1991 *J. Phys.: Condens. Matter* at press
- Skriver H L 1982 *Phys. Rev. Lett.* **49** 1768
- Slater J C and Koster G F 1954 *Phys. Rev.* **94** 1498
- Sutton A P, Finnis M W, Pettifor D G and Ohta Y 1988 *J. Phys. C: Solid State Phys.* **21** 35
- Turchi P and Ducastelle F 1985 *The Recursion Method and Its Applications (Solid State Sciences 58)* ed D G Pettifor and D L Weaire (Berlin: Springer) p 104
- Turchi P, Ducastelle F and Treglia G 1982 *J. Phys. C: Solid State Phys.* **15** 2891
- Yin M T and Cohen M L 1982 *Phys. Rev. B* **26** 5668